New Journal of Physics
The open access journal at the forefront of physics
Deutsche Physikalische Gesellschaft DPG | IOP Institute of Physics

Measuring topological invariants in small photonic lattices

C-E Bardyn[1,2], S D Huber[3] and O Zilberberg[3]
[1] Dept. of Physics, California Institute of Technology, Pasadena, CA 91125, USA
[2] Institute for Quantum Electronics, ETH Zurich, 8093 Zürich, Switzerland
[3] Institute for Theoretical Physics, ETH Zurich, 8093 Zürich, Switzerland
E-mail: cbardyn@caltech.edu and zilberberg@itp.phys.ethz.ch

Received 3 August 2014
Accepted for publication 27 October 2014
Published 8 December 2014
New Journal of Physics **16** (2014) 123013
doi:10.1088/1367-2630/16/12/123013

Abstract
We present a robust practical scheme for measuring the topological invariants of non-interacting tight-binding models realized in arrays of coupled photonic cavities. More specifically, we aim to focus on the implementation of a single unit cell with tunable twisted boundary conditions in order to access the bulk topological properties of much larger systems experimentally. We illustrate our method in a two-dimensional integer quantum Hall model, demonstrating that the associated topological invariants can be measured to a high degree of accuracy despite the driven-dissipative bosonic nature of the system, and discuss the robustness of our scheme against various sources of disorder.

Keywords: topological, photonic, quantum Hall

1. Introduction

Advances in the engineering of photonic crystals [1–4], coupled optical cavities [5, 6], and superconducting circuits [7–10] have made it possible to investigate fascinating aspects of condensed matter physics. This approach has faced its own challenges, however, since photons, as opposed to electrons, typically weakly interact and—most crucially—do not exhibit fermionic statistics. The technological difficulty of suppressing disorder in large arrays of photonic cavities as well as the unavoidable photon losses additionally constrain the

scalability of such systems, rendering the investigation of bulk properties particularly challenging.

Of recent interest in condensed matter physics are *topological* phenomena. In this active field of research, one typically deals with gapped systems such as band insulators and superconductors in which energy bands are characterized by non-trivial topological invariants, leading to remarkable observable phenomena [11, 12]. Although the study of topological phases originated in condensed matter physics, recent experiments involving photonic crystals [2, 4, 13–15] and arrays of coupled cavities [6] have opened up a similar avenue for research in photonic systems.

Bulk topological properties are properties of energy bands *as a whole* which are expected to manifest themselves through observable physical quantities when bands are *uniformly* populated. In fermionic systems, energy bands naturally fill up owing to the Pauli exclusion principle, leading to a variety of observable topological responses such as quantized Hall conductances in two-dimensional (2D) electron gases [16] and quantized magnetoelectric effects in 3D topological insulators [17]. Fermionic statistics is key to the observation of bulk topological properties in such cases, raising the intriguing question of how to observe similar properties in bosonic systems and in photonic ones, in particular.

In photonic systems, the lack of any exclusion principle combined with unavoidable photon losses makes it particularly challenging to populate energy bands uniformly. As a consequence, topological phenomena such as quantized Hall conductances—of great importance in bulk insulators—have no natural photonic counterpart. In addition, the associated current-carrying chiral edge states are necessarily affected by dissipation. It thus appears natural to ask whether the topological invariants associated with specific energy bands can at all give rise to robust *quantized* observable quantities. First steps in this direction were taken in two recent proposals based on edge state manipulations [18] and on the identification of optical responses providing approximate values of integer topological invariants [19].

In this work, we present a robust practical method to measure the bulk topological properties of photonic lattice systems. Our approach crucially relies on the realization of a small (unit-cell-sized) array of coupled cavities with tunable twisted boundary conditions. On the one hand, the restriction to a small system allows us to readily achieve some uniform band filling. On the other hand, the use of tunable twisted boundary conditions restores our ability to study larger systems with translation invariance [20, 21]. We illustrate the power and limitations of our scheme by investigating in detail a 2D integer quantum Hall (Hofstadter) model [22], demonstrating that the topological invariant (Chern number) characterizing the bands of such a model can be measured exactly, even in the presence of disorder.

2. Unit-cell photonic setup

We consider a generic non-interacting tight-binding (lattice) model

$$H = \sum_{i,j} a_i^\dagger \mathcal{H}_{ij} a_j, \tag{1}$$

where $a_i^\dagger$ (a_i) are operators creating (annihilating) particles on a lattice site i and $\mathcal{H}$ is an arbitrary first-quantized single-particle Hamiltonian. We wish to study the bulk properties of

this model by implementing it on a lattice of photonic cavities coupled via photon tunnelling. To this end, we assume that each lattice site i corresponds to a cavity supporting a single mode with resonance frequency $\mathcal{H}_{ii} = \omega_i$, and that photon tunnelling occurs between cavities i and j with amplitude $\mathcal{H}_{ij} = t_{ij} e^{i\phi_{ij}}$ where $t_{ij} > 0$ and $\phi_{ij} \in [0, 2\pi)$.

In practice, such a photonic realization does not perfectly capture the Hamiltonian dynamics of interest since—as in any photonic system—photon losses must be taken into account and compensated for by a drive. Assuming that photons are injected into the system using a monochromatic coherent driving field with frequency Ω, the relevant dynamics takes the form of a standard master equation in Lindblad form

$$\partial_t \rho = -i\big[H + H_{\text{drive}}, \rho\big] + \gamma \sum_i \Big(2a_i \rho\, a_i^\dagger - \big\{a_i^\dagger a_i, \rho\big\}\Big), \tag{2}$$

where ρ is the density matrix of the system, γ is the decay rate of the cavities (spatially uniform, for simplicity), and $H_{\text{drive}} = \sum_i (f_i e^{-i\Omega t} a_i + \text{H.c.})$ is the Hamiltonian of the drive involving the amplitude f_i of the driving field at the location of the ith cavity (note that $\hbar = 1$ here and in what follows).

Starting from empty cavities, the driven-dissipative dynamics described by (2) makes the system evolve to a state which is, at all times, a direct product of local coherent states. More specifically, each cavity i is found in a coherent state determined by a single complex parameter $\alpha_i \equiv \text{Tr}\,(\rho\, a_i)$ whose evolution is governed by the classical equation

$$i\partial_t |\alpha\rangle = \big(\mathcal{H} - \big(\Omega + i\gamma\big)\big)|\alpha\rangle + |f\rangle, \tag{3}$$

where we have introduced the Dirac vector notation $|x\rangle = (x_1, x_2, \ldots, x_N)$ and have moved to a rotating frame with frequency Ω by the transformation $e^{-i\Omega t}\alpha_i \to \alpha_i$. In steady state, the coherent cavity fields take the form

$$|\alpha\rangle = (\mathcal{H} - (\Omega + i\gamma))^{-1}|f\rangle = \sum_m \frac{\langle \psi_m | f\rangle}{\big(E_m - \Omega\big) + i\gamma}\, |\psi_m\rangle, \tag{4}$$

where $|\psi_m\rangle$ are the eigenstates of $\mathcal{H}$ with corresponding eigenenergies E_m.

Equation (4) is a standard result (see, for example, [23, 24]) which reflects the power and limitations of the photonic implementation introduced so far. It shows that the vector $|\alpha\rangle$ of coherent cavity fields corresponds, in steady state, to a superposition of eigenstates of the targeted Hamiltonian $\mathcal{H}$. Each eigenstate $|\psi_m\rangle$ contributes to the superposition according to (i) its spatial overlap $\langle\psi_m|f\rangle$ with the vector $|f\rangle$ of driving-field amplitudes and (ii) its Lorentzian response to the driving frequency Ω, with resonance frequency E_m and linewidth 2γ. More importantly, any eigenstate $|\psi_m\rangle$ can be addressed individually provided that the corresponding energy level E_m is separated by more than γ from the rest of the spectrum. Eigenstates that cannot be spectrally resolved (i.e., with energy separation $\Delta \ll \gamma$), instead, contribute to (4) with a relative weight solely determined by their spatial overlap with the driving field. This reflects an important limitation of photonic realizations of Hamiltonian models, namely, the fact that energy bands do not automatically fill in a uniform way as in fermionic systems where the Pauli exclusion principle prevails.

To circumvent the issue of non-uniform filling, we intend to investigate the bulk properties of a large system focusing on a *single unit cell*. To this end, we assume that the non-

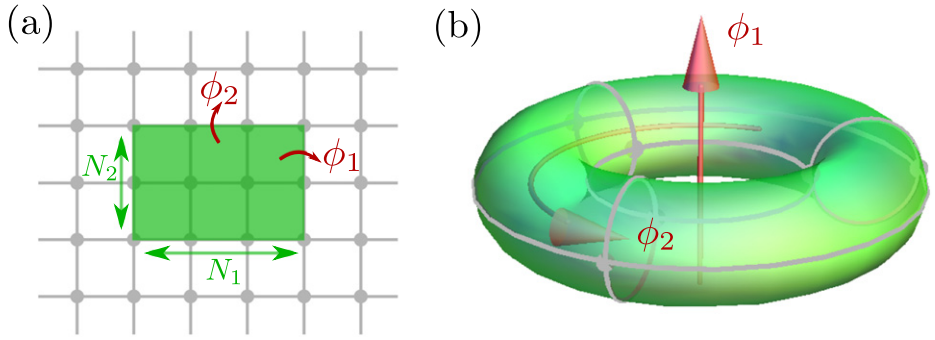

Figure 1. Unit cell of interest. (a) Unit-cell configuration consisting of N_u lattice sites in each spatial direction $u = 1, 2$ (in 2D) with twisted boundary conditions defined by periodic boundary conditions with additional twist angles ϕ_u at the boundaries. (b) Gauge-equivalent configuration with periodic boundary conditions and fluxes ϕ_u threading the unit cell.

interacting tight-binding model of interest (defined in (1)) is translationally invariant with respect to an enlarged unit cell of N lattice sites consisting of N_u sites in each spatial direction u[4]. For simplicity—and without loss of generality—we focus on 2D models so that $u = 1, 2$ and $N = N_1 \times N_2$. Using Bloch's theorem, the large system that we wish to investigate can be described in momentum space by an $N \times N$ Hamiltonian $\mathcal{H}(\mathbf{k})$ and thus exhibits up to N energy bands $E_n(\mathbf{k})$ with associated eigenstates $|\psi_n(\mathbf{k})\rangle$, where $\mathbf{k} = (k_1, k_2)$ with $k_u \in [-\pi/N_u, \pi/N_u]$ and n is the index of the band. Crucially, one can equivalently investigate the Hamiltonian $\mathcal{H}(\mathbf{k})$ in a unit-cell array of N coupled photonic cavities by encoding the momentum $\mathbf{k}$ in *twisted* boundary conditions [20, 21], i.e., periodic boundary conditions with an additional directional phase shift (or 'twist angle') $\pm N_u\phi_u$ for tunnelling across the boundary of the system in each direction u (see figure 1). Physically, this stems from the fact that the phase $N_u\phi_u$ picked up by photons upon tunnelling across the unit cell in a direction u can be identified with the phase $N_u k_u$ accumulated, in an infinite system, by a plane wave $e^{i\mathbf{k}\cdot\mathbf{r}}$ travelling across a unit cell in the same direction ($\mathbf{r}$ being the position vector). In the following, we shall therefore denote both the twist angles and the momentum by $\boldsymbol{\phi} = (\phi_1, \phi_2)$, i.e., $\boldsymbol{\phi} \equiv \mathbf{k}$.

In light of the above discussion, unit-cell photonic implementations provide two major advantages: (i) Since each energy band generically reduces to a single state, a high spectral resolution is readily achieved: Provided that $\mathcal{H}(\boldsymbol{\phi})$ is gapped and that the photon loss rate γ is much smaller than the minimal gap, the frequency Ω of the driving field can be tuned into resonance with any targeted eigenstate $|\psi_n(\boldsymbol{\phi})\rangle$, thereby giving rise to steady-state coherent cavity fields $|\boldsymbol{\alpha}\rangle \approx |\psi_n(\boldsymbol{\phi})\rangle$ (i.e., the sum in (4) reduces to one term), up to an irrelevant complex factor[5]. In other words, the eigenstates $|\psi_n(\boldsymbol{\phi})\rangle$ of the Hamiltonian $\mathcal{H}(\boldsymbol{\phi})$ of interest can be *observed* by measuring the amplitude and phase of the light emitted in steady state by each of the N cavities of the unit-cell photonic lattice. Similarly, the spectrum $E_n(\boldsymbol{\phi})$ can be measured using standard optical spectroscopy techniques—by monitoring, e.g., the total number of

[4] Note that the invariance of the Hamiltonian under translations is gauge dependent since the phases ϕ_{ij} appearing in (1) are gauge-dependent quantities. Here we assume that a suitable gauge has been chosen.

[5] We assume, without loss of generality, that the spatial overlap $\langle\psi_n(\boldsymbol{\phi})|f\rangle$ between the targeted eigenstate and the vector of driving-field amplitudes is finite.

photons transmitted into the system as a function of the frequency Ω of the driving field. (ii) The ease with which the twist angles $\boldsymbol{\phi}$ can in principle be tuned in photonic systems—by modifying the optical path lengths through which the cavities are coupled across the boundaries of the system—makes it possible to investigate the bulk properties of arbitrarily large systems[6] using a much smaller (unit-cell) system size. Additionally, it provides a way to investigate large non-interacting quantum systems in an intrinsically *momentum-resolved* manner[7].

We remark that the unit cell of interest must have at least two lattice sites in each spatial direction (i.e., $N_u \geqslant 2$ for all u) in order for our scheme to work without further modifications, since twist angles ϕ_u can only be introduced in the photon tunnelling between *distinct* sites. We emphasize, however, that this is not a fundamental constraint: If $N_u = 1$ for a particular direction u, one can always introduce the required twist angle ϕ_u by modulating, instead, the resonance frequencies ω_i of the cavities [2, 3, 14, 25], as exemplified in the next section. In any case, tunable twisted boundary conditions and resonance frequencies can both be realized in photonic systems using standard techniques. In particular, modulated on-site resonance frequencies have been implemented in the context of photonic lattices [2], and the realization of tunable twisted boundary conditions has been discussed in detail in the context of arrays of coupled optical cavities [18].

3. Illustrative example: integer quantum Hall effect

The unit-cell photonic setup introduced above provides a direct way to *measure* both the spectrum and the wavefunctions of any targeted gapped non-interacting Hamiltonian with translation invariance, allowing us to extract all of its bulk properties. Bulk topological properties, in particular, can be accessed through momentum-resolved measurements of the gauge-invariant spectral projection operator [26–28]

$$P_n(\boldsymbol{\phi}) = \left|\psi_n(\boldsymbol{\phi})\right\rangle\left\langle\psi_n(\boldsymbol{\phi})\right|, \tag{5}$$

which is to be contrasted with previous proposals allowing us to probe topology in photonic lattices through the observation of edge states [18], approximate responses [19] or so-called 'Zak phases' [29].

Below we demonstrate that the precise integer value of the topological invariants found in 2D integer quantum Hall systems described by the Hofstadter model [22] can be measured in a robust way in our proposed unit-cell photonic setup. The Hofstadter Hamiltonian describes non-interacting particles hopping on a square lattice under a (real or synthetic) uniform perpendicular magnetic field, and takes a similar form as the generic Hamiltonian (1), namely,

$$H_{\text{Hofstadter}} = t\sum_{\langle i,j\rangle} a_i^\dagger a_j e^{i\phi_{ij}}, \tag{6}$$

with a uniform hopping amplitude $t > 0$ and vanishing on-site potentials (the sum being restricted to the nearest-neighboring sites). Although the phases ϕ_{ij} are gauge-dependent quantities, the phase $\phi_p = \sum_p \phi_{ij}$ accumulated when hopping once around an elementary square

[6] The maximum system size that can be investigated in the unit-cell implementation of interest is limited by (i) the resolution that can be achieved for varying the twist angles, and (ii) the broadening of the energy levels due to photon losses.

[7] Note that momentum-resolved spectroscopy can also be achieved in a finite system with open boundary conditions by focusing a pump laser beam at a specific angle over a wide area.

(or 'plaquette') of the lattice in the counter-clockwise direction is gauge-independent and physically corresponds to an effective magnetic field. Here we assume that the number $n_p = (2\pi)^{-1}\phi_p$ of magnetic flux quanta per plaquette is constant and rational, i.e., $n_p = p/q$ with co-prime integers p and q, so that the corresponding effective magnetic field is uniform and commensurate with the lattice. The Hamiltonian is then translationally invariant with respect to a so-called 'magnetic' unit cell which contains q lattice sites [20, 21, 30, 31]. More importantly, the infinite system that we wish to investigate generically exhibits q energy bands with non-trivial topological properties: Each band n is characterized by an integer topological invariant known as the (first) Chern number [20, 21, 30], defined as

$$\nu_n = \frac{1}{2\pi \mathrm{i}} \int_0^{2\pi} \mathrm{d}\phi_1 \int_0^{2\pi} \mathrm{d}\phi_2 \, \mathrm{Tr}\left(P_n\left[\partial_{\phi_1} P_n, \partial_{\phi_2} P_n\right]\right), \tag{7}$$

where $P_n = P_n(\phi_1, \phi_2)$ is the spectral projection operator associated with the band of interest (see equation (5)). This Chern number is a topological property of an entire band which manifests itself most readily in fermionic systems where each band n contributes, when filled, to the overall Hall conductance by an integer value corresponding to its Chern number ν_n (in units of e^2/h) [20, 21, 30].

To investigate the Hofstadter model in a unit-cell photonic setup, the first step is to engineer a photonic lattice system described by the corresponding Hamiltonian (see equation (6)), restricting the system to a single magnetic unit cell of size $N_1 \times N_2$ with twisted boundary conditions and tunable twist angles ϕ_1 and ϕ_2. We remark that N_1 and N_2 can be modified at will by a suitable choice of gauge (i.e., of phases ϕ_{ij} in (6)) provided that $N_1 \times N_2 = q$[8]. If $N_1, N_2 \geqslant 2$, both twist angles can be introduced as tunnelling phase shifts as discussed above. If $N_u = 1$ in some direction u, however, the corresponding twist angle ϕ_u must be encoded through modulated on-site potentials. Below we numerically investigate two cases exemplifying both of these scenarios.

3.1. Encoding phase twists in tunnelling phases

We start by examining the generic case $n_p = p/q$ where q is not a prime number, in which there always exists a gauge such that $N_1, N_2 \geqslant 2$ and all twist angles can be introduced as tunnelling phases. We focus on the example $n_p = 1/6$ and choose a gauge in which the (magnetic) unit cell has dimensions 3×2 (see figure 2(a)). The unit-cell photonic system exhibits 6 energy levels, as expected. Note that these levels correspond to five bands, as two of them form a single band as a function of the twist angles (ϕ_1, ϕ_2) (see figure 2(b)). Most importantly, the spectral projector $P_n(\phi_1, \phi_2)$ associated with a particular band n can be *measured* for all values of ϕ_1 and ϕ_2 at which the energy level(s) forming the band of interest are spectrally resolvable despite the broadening due to photon losses with rate γ. For bands formed by a single energy level and separated by a gap Δ from the rest of the spectrum, $\gamma \ll \Delta$ is the only requirement. Once measurements of $P_n(\phi_1, \phi_2)$ have been performed for a discrete set of values $\phi_1, \phi_2 \in [0, 2\pi)$, the Chern number ν_n of the corresponding band can be extracted using its very definition, i.e., using a discretized version of (7). We note that in most cases a coarse sampling of $P_n(\phi_1, \phi_2)$ over the 'Brillouin zone' (ϕ_1, ϕ_2) is sufficient to determine the value of ν_n correctly [32]. We

[8] Note that the gauge is fixed at the level of the physical implementation, since gauge invariance is broken by dissipation (photon losses).

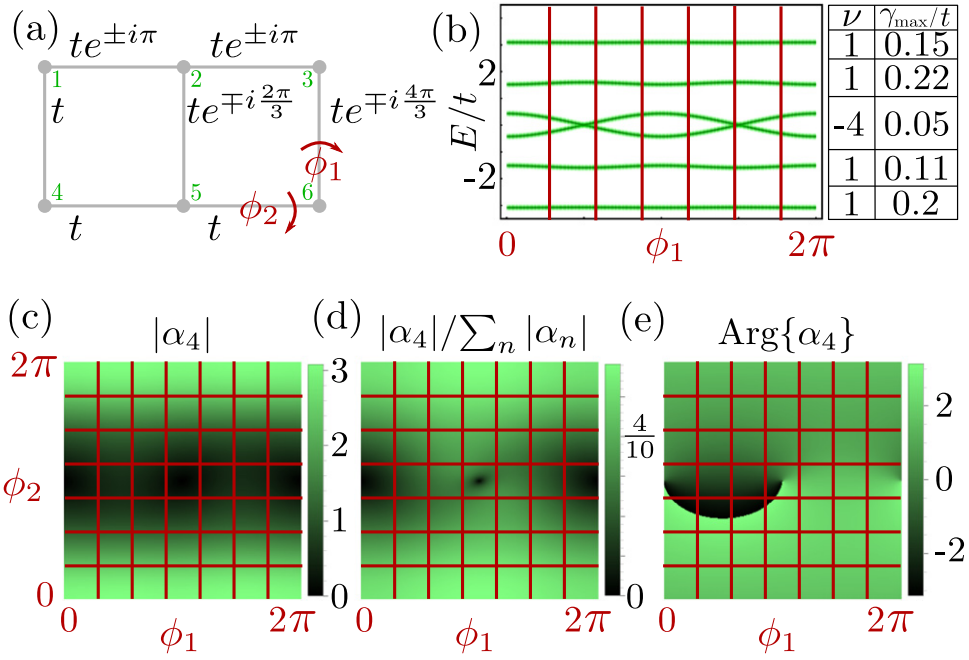

Figure 2. Unit-cell photonic implementation of a 2D quantum Hall-like Hofstadter model with $n_p = p/q = 1/6$ effective magnetic flux quanta per (square-lattice) plaquette. (a) Relevant (magnetic) unit cell containing $q = 6$ lattice sites, with uniform hopping amplitudes t and hopping phases ϕ_{ij} (or gauge; see (6)) chosen here so that $N_1 = 3$, $N_2 = 2$. Twisted boundary conditions are indicated by the corresponding twist angles ϕ_1 and ϕ_2. (b) Left: spectrum $E(\phi_1, \phi_2)$ (shown here as a function of ϕ_1 with $\phi_2 = 0$) exhibiting $q = 6$ energy levels which generate the bands of the infinite system of interest as the twist angles are continuously varied. Right: table presenting the Chern number ν extracted for each band using a coarsely discretized (7×7 grid) twist-angle space, along with the (estimated) maximum photon loss rate $\gamma_{\max}$ allowing us to extract it. Note that $\gamma_{\max}$ is much smaller for the central band because the latter consists of 2 energy levels which must be spectrally resolvable—for all chosen values of ϕ_1 and ϕ_2—for our scheme to work. (c) From left to right: steady-state coherent-field amplitude, normalized amplitude, and phase found in cavity 4 (see (a)) as a function of the twist angles (also shown is the 7×7 discretization grid that is used). All three plots were obtained for $t = 1$ and $\gamma = 0.1$. The driving was applied to cavity 1 with a coherent field amplitude $f = 1$ and frequency Ω tuned into resonance with the lowest energy level $E(\phi_1, \phi_2)$ (see (b)).

present in figure 2(b) a table showing the values of ν_n that would be correctly measured for each of the bands using a 7×7 sampling grid, along with the maximum photon loss rate $\gamma_{\max}$ allowed for a correct measurement. Figures 2(c)–(e) illustrate the typical data that must be obtained, for each cavity, in order to extract the Chern number of a specific band.

3.2. Encoding phase twists in modulated on-site potentials

We now turn to the generic situation $n_p = p/q$ where q is a prime number, in which case there exists no gauge in which $N_1, N_2 \geqslant 2$ is satisfied and at least one of the required twist angles must be encoded, e.g., through modulated on-site potentials. In that case the idea is to investigate the model of interest in a mixed position–momentum representation. Here we

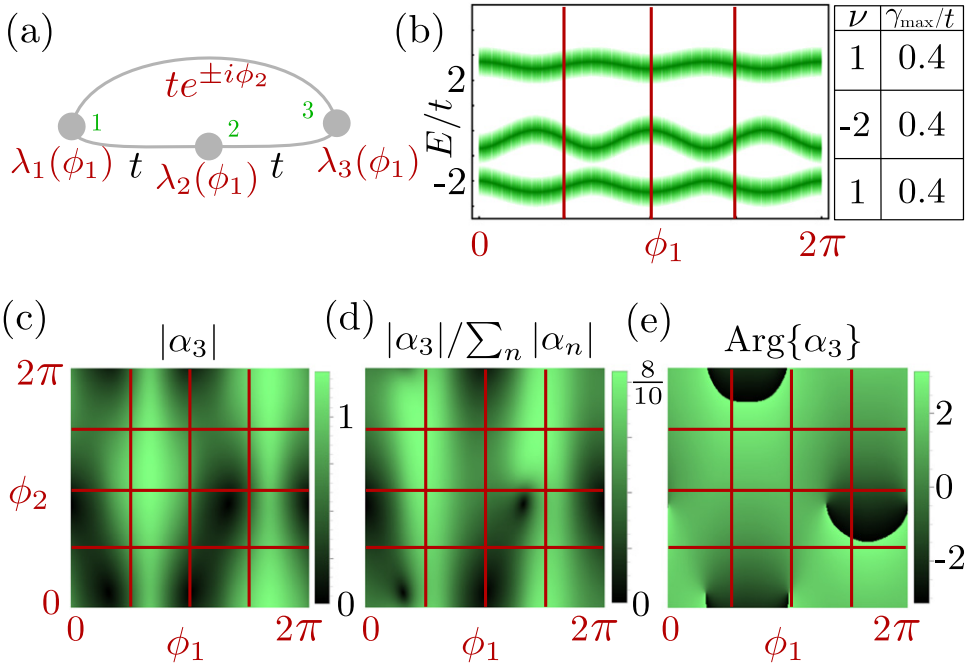

Figure 3. Unit-cell photonic implementation of an infinite quantum Hall-like system with $n_p = p/q = 1/3$ effective magnetic flux quanta per (square-lattice) plaquette. We use a mixed position-Fourier representation in order to treat the case $q = 3$ where q is prime. (a) Relevant unit cell of the Harper model containing $q = 3$ lattice sites, with uniform hopping amplitudes t and modulated on-site potential (see equation (8)). Twisted boundary conditions are indicated by the corresponding twist angles ϕ_1 and ϕ_2. (b) Left: spectrum $E(\phi_1, \phi_2)$ (shown here as a function of ϕ_1 with $\phi_2 = 0$) exhibiting $q = 3$ energy levels generating the bands of the infinite system of interest as the twist angles are continuously varied. Right: table indicating the Chern number ν extracted for each band using a coarsely discretized (4×4 grid) twist-angle space, along with the (estimated) maximum photon loss rate $\gamma_{\max}$ allowing us to extract it. (c) From left to right: steady-state coherent-field amplitude, normalized amplitude, and phase obtained in cavity 3 (see (a)) as a function of the twist angles (showing the 4×4 discretization grid that is used). All three plots were obtained for $t = 1$ and $\gamma = 0.4$, driving cavity 1 with a coherent field of amplitude $f = 1$ and frequency Ω tuned into resonance with the central energy level $E_2(\phi_1, \phi_2)$ (see (b)).

choose the Landau gauge and write the Hofstadter Hamiltonian (6) in the form

$$H = t\sum_{m,n}\left(a^{\dagger}_{n,m+1}a_{n,m} + a^{\dagger}_{n+1,m}a_{n,m}e^{i2\pi n_p m} + \text{H.c.}\right)$$
$$= t\sum_{m,k}\Big[\left(a^{\dagger}_{m+1,k}a_{m,k} + \text{H.c.}\right) + 2\cos\left(2\pi n_p m + k\right)a^{\dagger}_{m,k}a_{m,k}\Big], \tag{8}$$

where, in the last equality, we have performed a Fourier transform in the spatial direction indexed by n. The resulting position–momentum representation corresponds to a family of Harper models [33]. We recall that our aim is to investigate the bulk properties of the original model by modifying twist angles corresponding, in the unit cell, to different momenta. Replacing $k \to \phi_1$ in (8), the twist angle associated with the direction indexed by n is here encoded in the on-site potential of a 1D Harper model. This corresponds, in a unit-cell setup, to a modulation of the resonance frequencies ω_i of the individual cavities [2]. The second twist

angle ϕ_2, on the other hand, can be introduced as twisted boundary conditions (i.e., as a tunnelling phase) in the remaining spatial direction.

As an example, we investigate the case $n_p = 1/3$ numerically (see figure 3(a)). The unit-cell photonic system exhibits, as expected, $q = 3$ energy levels (see figure 3(b)). As in the previous example, the Chern number ν_n of each band n can be extracted in a robust way by measuring $P_n(\phi_1, \phi_2)$ for a discrete set of values $\phi_1, \phi_2 \in [0, 2\pi)$. Here we use a coarse 4×4 grid for sampling $P_n(\phi_1, \phi_2)$ over the 'Brillouin zone' (ϕ_1, ϕ_2) [32]. Figure 3(b) shows a table presenting the values of ν_n that would be correctly measured for each of the bands, along with the maximum photon loss rate $\gamma_{\max}$ allowed for a correct measurement. Figures 3(c)–(e) illustrate the typical data that must be measured, for each cavity, in order to extract the Chern number of a specific band.

In a Hamiltonian system, the Chern number can be evaluated in a robust way in the presence of on-site and hopping disorder provided that any gap Δ separating the band of interest from the rest of the spectrum remains open. There are two important differences in our experimental proposal: (i) additional sources of disorder are present, namely, fluctuations in the driving frequency, inhomogeneous and fluctuating cavity decay rates, and an uneven sampling of the (ϕ_1, ϕ_2) space; (ii) the spectral gaps are effectively smaller due to the linewidth 2γ. We have studied numerically the robustness of our scheme against all expected sources of disorder: As long as the disorder strength is much weaker than $\Delta - 2\gamma$, the obtained Chern numbers are invariant and correct. When disorder of the order of $\gamma_{\max}$ is introduced for the cavity decay rates, a wrong integer may be obtained.

4. Conclusion

We have proposed a robust practical scheme to measure topological invariants in non-interacting photonic lattice systems despite their driven-dissipative bosonic nature and the presence of disorder. As a demonstration of our method, we have shown that integer topological invariants can in principle be measured to a high degree of accuracy in a minimum setting of as few as three tunnel-coupled optical cavities.

We anticipate that our proposal will allow for the observation of a variety of bulk topological properties that have only been theoretically predicted so far, such as topological phenomena protected by spatial symmetries [34–37]. Indeed, the fact that translation invariance is intrinsically preserved in our proposed unit-cell implementation provides access to a rich variety of symmetry-protected topological classes [26–28, 34–38]. Both spatial and non-spatial symmetries can in principle be introduced by suitably engineering the underlying photonic system [10].

We expect the concept of unit-cell photonic implementation introduced in this work to prove useful in the investigation of bulk properties other than topological invariants. Our proposal ultimately relies on two essential ingredients: (i) the restriction to small photonic lattice systems in order to achieve a high spectral resolution, and (ii) the use of tunable twisted boundary conditions to probe different momentum sectors. One important future direction will be to apply similar ideas to study (small) photonic lattice systems with interactions.

Acknowledgments

The authors would like to thank M Hafezi for motivating this endeavor, A İmamoğlu and G Blatter for their support, and G-M Graf, A Srivastava, and E van Nieuwenburg for fruitful

discussions. Financial support from the Swiss National Science Foundation (SNSF) is also gratefully acknowledged.

References

[1] Lahini Y, Pugatch R, Pozzi F, Sorel M, Morandotti R, Davidson N and Silberberg Y 2009 *Phys. Rev. Lett.* **103** 013901
[2] Kraus Y E, Lahini Y, Ringel Z, Verbin M and Zilberberg O 2012 *Phys. Rev. Lett.* **109** 106402
[3] Verbin M, Zilberberg O, Kraus Y E, Lahini Y and Silberberg Y 2013 *Phys. Rev. Lett.* **110** 076403
[4] Rechtsman M C, Zeuner J M, Plotnik Y, Lumer Y, Podolsky D, Dreisow F, Nolte S, Segev M and Szameit A 2013 *Nature* **496** 196–200
[5] Hafezi M, Demler E, Lukin M and Taylor J 2011 *Nat. Phys.* **7** 907–12
[6] Hafezi M, Mittal S, Fan J and Taylor J M 2012 *Nat. Photonics* **7** 1001–5
[7] Houck A A, Türeci H E and Koch J 2012 *Nat. Phys.* **8** 292–9
[8] Underwood D L, Shanks W E, Koch J and Houck A A 2012 *Phys. Rev.* A **86** 023837
[9] Schmidt S and Koch J 2013 *Ann. Phys., Lpz.* **525** 395–412
[10] Jia N, Sommer A, Schuster D and Simon J 2013 (arXiv:1309.0878)
[11] Hasan M Z and Kane C L 2010 *Rev. Mod. Phys.* **82** 3045–67
[12] Qi X L and Zhang S C 2011 *Rev. Mod. Phys.* **83** 1057–110
[13] Wang Z, Chong Y, Joannopoulos J D and Soljacic M 2009 *Nature* **461** 772–5
[14] Kraus Y E and Zilberberg O 2012 *Phys. Rev. Lett.* **109** 116404
[15] Verbin M, Zilberberg O, Lahini Y, Kraus Y E and Silberberg Y 2014 (arXiv:1403.7124)
[16] Klitzing K V, Dorda G and Pepper M 1980 *Phys. Rev. Lett.* **45** 494–7
[17] Qi X L, Hughes T L and Zhang S C 2008 *Phys. Rev.* B **78** 195424
[18] Hafezi M 2014 *Phys. Rev. Lett.* **112** 210405
[19] Ozawa T and Carusotto I 2014 *Phys. Rev. Lett.* **112** 133902
[20] Thouless D J, Kohmoto M, Nightingale M P and den Nijs M 1982 *Phys. Rev. Lett.* **49** 405–8
[21] Avron J E, Seiler R and Simon B 1983 *Phys. Rev. Lett.* **51** 51–3
[22] Hofstadter D R 1976 *Phys. Rev.* B **14** 2239–49
[23] Umucalilar R O and Carusotto I 2011 *Phys. Rev.* A **84** 043804
[24] Umucalilar R O and Carusotto I 2012 *Phys. Rev. Lett.* **108** 206809
[25] Kraus Y E, Ringel Z and Zilberberg O 2013 (arXiv:1308.2378)
[26] Altland A and Zirnbauer M R 1997 *Phys. Rev.* B **55** 1142–61
[27] Schnyder A P, Ryu S, Furusaki A and Ludwig A W W 2008 *Phys. Rev.* B **78** 195125
[28] Ryu S, Schnyder A P, Furusaki A and Ludwig A W W 2010 *New J. Phys.* **12** 065010
[29] Longhi S 2013 *Opt. Lett.* **38** 3716–19
[30] Kohmoto M 1985 *Ann. Phys.* **160** 343–54
[31] Dana I, Avron Y and Zak J 1985 *J. Phys. C: Solid State Phys.* **18** L679
[32] Fukui T, Hatsugai Y and Suzuki H 2005 *J. Phys. Soc. Japan* **74** 1674–7
[33] Harper P G 1955 *Proc. Phys. Soc.* A **68** 874
[34] Fu L 2011 *Phys. Rev. Lett.* **106** 106802
[35] Hsieh T H, Lin H, Liu J, Duan W, Bansil A and Fu L 2012 *Nat. Commun.* **3** 982
[36] Tanaka Y, Ren Z, Sato T, Nakayama K, Souma S, Takahashi T, Segawa K and Ando Y 2012 *Nat. Phys.* **8** 800–3
[37] Okada Y *et al* 2013 *Science* **341** 1496–99
[38] Kitaev A 2009 *AIP Conf. Proc* **1134** 22–30